# On the flow characteristics of normal and inclined square jets in cross-flow: a numerical study

MOHAMED MAIDI and YUFENG YAO
Faculty of Engineering
Kingston University
Roehampton Vale, Friars Avenue, London, SW15 3DW
UNITED KINGDOM
http://www.kingston.ac.uk

*Abstract:* - Numerical simulation has been performed by solving full Navier–Stokes equations governing the three-dimensional unsteady compressible flows. The main goal of the present work is to investigate the flow characteristics of a square jet issuing transversally into a cross-flow at three injection angles of 90°, 60° and 30°, and thus to provide some deeper insights into the physical flow mechanism governing the normal and inclined jets in cross-flow. The simulation uses the jet to cross-flow velocity ratio of 2.5 and the Reynolds number based on the free-stream quantities and the jet exit diameter is 225. While the vortical structures predicted from the normally jet were in good qualitatively agreement with the findings of other researchers, our simulations have shown that both the jet penetration and jet cross-flow mixing are strongly dependent on the jet inclination angle. As expected, the jet spreading angle and penetration depth are observed to be greatest from the normal jet case. It has also found from the simulations that the streamwise jet inclination weakens significantly the cross-flow entrainment into the near wake region. These observations and information are of great practical relevance notably for cooling system of turbine blades designer.

*Key-Words:* - Direct numerical simulation, Jets in cross-flow, Vortex structures, Jet penetration and spreading, Cross-flow entrainment.

## 1 Introduction

The behavior of a normal jet in a cross-flow (JICF) has been extensively investigated due to its wider engineering and industrial applications involving mixing and pollutant dispersion from chimney stacks, film cooling of turbine blades, V/STOL aircraft and numerous manufacturing processes. An extensive review was given by Margason [1], covering fifty years of JICF researches up to 1993.

Fric and Roshko [2] observed the complex vortex system associated with JICF and described the findings with four main vertical structures, namely the horseshoe vortices, the jet shear layer vortices, the wake vortices, and the counter rotating vortex pairs (see Fig.1). The horseshoe vortices form upstream of the jet exit and wrapping around the exiting jet orifice. The jet shear layer consists of the vortex rollers in the upstream side of the jet. The wake structures form downstream of the jet column, which persist and convectively transport to further downstream of the exit nozzle. The counter-rotating vortex pair (CRVP) which is originated as an effect of the bending of the jet itself constitutes the dominant structure of the vortex system. These observations were also confirmed by other researcher, e.g., Smith *et al.* [3], Smith and Mungal [4], Lozano *et al*. [5], Eiff *et al*. [6]. In these studies, a major parameter used for characterizing the jet in a cross-flow is the ratio of the jet momentum to the cross-flow momentum, *R*. The wake vortices are observed for large momentum ratios while the CRVP is the dominant structure for all range of velocity ratio.

Despite the fact that the inclined jets are widely used in blade film cooling applications, there have been relatively few investigations of flow structure. Lee *et al*. [7] have experimentally studied the flow characteristics of streamwise inclined jets, injected at angle of 35° into a turbulent cross-flow boundary layer for two velocity ratios of 1.0 and 2.0. They demonstrated that a slight variation of the injection angle could produce significant changes in the flow structure. Lozano *et al.* [5] used the time-averaged images for identifying the centreline jet trajectory and the instantaneous images for the jet structures. However, further details are needed, notably at different injection angles. Film cooling effectiveness has been experimentally studied by Yuen and Martinez-Botas [8] on a cylindrical hole at three

streamwise inclination angles of 30°, 60° and 90°. They observed that at a velocity ratio of 0.33 the maximum effectiveness (in term of heat transfer between the cool jet flow and the hot cross-flow near the wall surface) in the near jet region has been achieved by the 30° hole, which was approximately 20% higher than that by two steeper (60° and 90°) holes.

While recent experiments have shed some new lights upon the effects of large-scale structures in the JICF configuration, many questions remain unanswered. Numerical simulations can provide certain details of complex flow structures and their interactions, but most simulations to date have been unable to accurately reproduce the entire flow behavior. In recent years, with the advance in numerical method and parallel computing power, it becomes possible to perform precise "numerical experiments" via the so-called direct numerical simulation (DNS), and to use the resultant database to extract information, which is often difficult or sometime even impossible to obtain at the laboratory conditions.

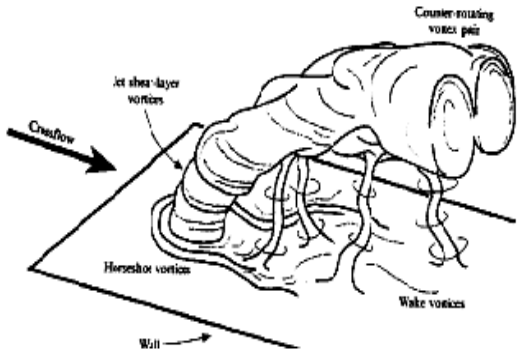


Fig.1: The vortex system in JICF (from Fric and Roshko [2]).

The present paper aims to investigate the effect of the jet inclination angle on the dynamical evolution of vertical structures associated with jet in cross-flow by direct numerical simulation. A multi-block parallel in-house solver is used to simulate the vertical flow development around a square jet issuing vertically into a cross-flow at three successive streamwise inclination angles of $30^o$, $60^o$, and $90^o$. In order to preserve the essence of the realistic flow nature, computation has performed in the full physical domain with highly refined uniform grids, and notably the present simulation reproduced all the experimentally observed flow features, as reported by Fric and Roshko [2], and Eiff *et al*. [6].

# 2 Numerical Method

## 2.1 Governing equations

The governing equations are the 3D compressible Navier-Stokes equations representing conservation laws for mass, momentum and energy in the Cartesian coordinates ($x$, $y$, $z$). By using reference values at free-stream, the non-dimensional form of the Navier-Stokes equations can be written as

$$\frac{\partial \rho}{\partial t} + \frac{\partial \rho u_i}{\partial x_i} = 0 , \tag{1}$$

$$\frac{\partial \rho u_i}{\partial t} + \frac{\partial \rho u_i u_j}{\partial x_j} = -\frac{\partial p}{\partial x_i} + \frac{1}{\mathrm{Re}} \frac{\partial \tau_{ij}}{\partial x_j} , \tag{2}$$

$$\frac{\partial E}{\partial t} + \frac{\partial (E+p) u_j}{\partial x_j} = -\frac{\partial q_j}{\partial x_j} + \frac{1}{\mathrm{Re}} \frac{\partial u_i \tau_{ij}}{\partial x_j} , \tag{3}$$

where $\rho$ is the density, $u_i$ the velocity components, $p$ the thermodynamic pressure, $E$ the total energy, $\tau_{ij}$ the shear stress tensor, $q_i$ the heat flux vector, and the Reynolds number $\mathrm{Re} = U_\infty D / \nu$ based on the free-stream velocity $U_\infty$ and the jet width $D$.

Assuming thermally perfect gas, the shear stress $\tau_{ij}$ and heat flux $q_i$ can be written as

$$\tau_{ij} = \mu \left( \frac{\partial \rho u_i}{\partial x_j} + \frac{\partial \rho u_j}{\partial x_i} - \frac{2}{3} \frac{\partial \rho u_k}{\partial x_k} \delta_{ij} \right), \tag{4}$$

$$q_j = \frac{-\mu}{(\gamma - 1)\mathrm{Pr}\,\mathrm{Re}\, M^2} \frac{\partial T}{\partial x_j}, \tag{5}$$

where the viscosity $\mu$ is specified through the power law ($\mu = T^\Omega$ with $T$ the non-dimensional temperature and $\Omega$ is a constant which equals to 0.76 for air) and the Prandtl number $Pr$ is set to 0.72.

## 2.2 Numerical technique

The above 3D compressible unsteady Navier-Stokes equations are numerically solved by using high-order finite-differences in space and multi-stage Runge-Kutta algorithm for time advancement. An entropy splitting concept is used to improve the stability of the numerical scheme, and stable boundary treatment technique is adopted at the boundaries. The code has been parallelized using the MPI library and validated extensively for numerous

configurations including laminar and turbulent boundary layers and plain channel flows ([9, 10]).

# 3 Problem Configuration

The problem configuration used in the simulations consists of a jet issuing from a rectangular duct pipe into a cross-flow at a given streamwise inclination angle. For all simulations, the computational box combines a rectangular cross-flow domain of with a dimension of 24D×8D×6D in longitudinal, wall-normal and transverse directions, respectively, and a duct jet domain of 1D×1D×1D, with D the jet width. The upper surface of the jet domain is joined with the bottom surface of the cross-flow domain. The jet is located in [4D, 5D] from the cross-flow inlet plane in the streamwise direction and [2.5D, 3.5D] in the spanwise direction, respectively. The computational grid has 241 points in the streamwise (with 11 points in the jet domain), 91 points in the wall-normal (with 81 points in the cross-flow domain and 11 points in the jet domain), and 61 points in the spanwise direction (with 11 points in the jet domain). The cross-flow velocity profile is initialized using a similarity solution of laminar boundary-layer at same Reynolds number and a Poiseuille-type profile is given at the inlet of jet orifice. The characteristics boundary conditions are used at both outlet plane and upper surface, and periodic conditions for the side-walls. Simulations are performed for a jet to cross-flow velocity ratio $R$ = 2.5 and a Reynolds number $Re$ = 225, based on the free-stream quantities of the cross-flow and the jet width (D). The low Reynolds number used in this investigation permits the clear observation of large-scale structures dynamics, which are difficult to study at high Reynolds number regime.

# 4 Results and Discussions

In the present study we present simulation results only at a particular instantaneous time of $t$ = 15. Results from normal JICF presented first, followed by the inclined JICF. Discussions are focused on the physical mechanism of JICF.

## 4.1 Normal jet in cross-flow

Detailed flow structures and vortex system evolving from the interactions of normal jet with mainstream cross-flow were presented.

In Fig. 2, we depict the spanwise vorticity ($\omega z$) contours on the z = 3D plane. The important flow feature which characterizes the interaction between the jet and the cross-flow is the formation of streamwise CRVP which dominates the flow field. In agreement with previous experimental and numerical predictions [11] [12], the CRVP was observed to originate from the two lateral jet boundary layers within the square duct and to persist far downstream. These coherent structures constitute an obstacle and generate adverse pressure gradients which produce horse-shoe vortices that wrap around the edge of the jet hole (see Fig. 3 and Fig. 8a). Fig.2 (and also Fig.6a) reveals the presence of the Kelvin–Helmholtz rollers (i.e., shear layer vortices) those emerge at the upstream side of the initial portion of the jet. The roll-up process of the shear layer upstream of the jet has been attributed to Kelvin-Helmholtz instabilities. It is worth mentioning that Fig. 2 does not show any indication of the presence of the Kelvin–Helmholtz rollers along the downstream side of the jet. This can be confirmed by Fig. 4 which gives streamline plots of two successive Kelvin–Helmholtz rollers. In agreement with DNS results of Sau *et al*. [12], this visualization reveals that the Kelvin–Helmholtz vortices did not grow in the form of closed loop (ring-like) structures around the jet. A closer view of the region near the jet exit is presented in Fig. 5. The streamline pattern shows the presence of another vortex structure just above the jet exit, near the leading edge. This vortex structure called "hovering vortex" and has been experimentally identified by Kelso *et al.* [13] at velocity ratio $R$ = 2.3. Downstream of the jet hole exit, Fig.2 shows also the shedding of so-called upright wake vortices from the downstream cross-flow shear layer. These vertically oriented vortices connect the jet body with the wall boundary layer. All these observations are in good agreement with experimental observations of Lim *et al.* [11], Kelso *et al*. [13] and DNS of Sau *et al*. [12].

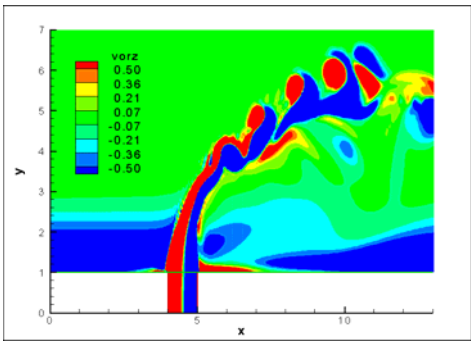


FIG 2: Contours of spanwise vortices $\omega_z$ on the vertical (x, y, z = 3D) plane.

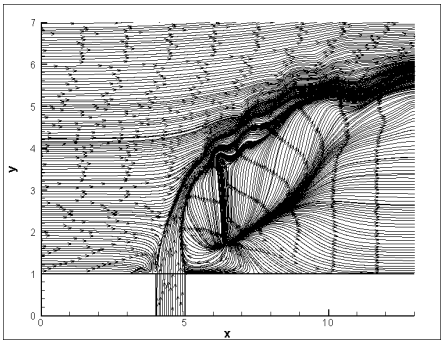


FIG 3: Streamline patterns on the vertical plane (x, y, z=3D).

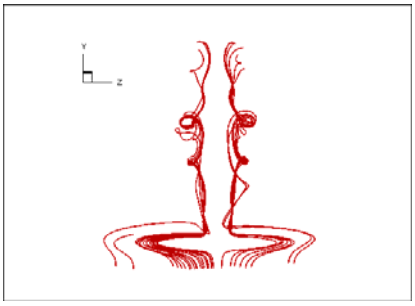

FIG 4: Three-dimensional streamlines revealing evolution pattern of Kelvin-Helmholtz rollers.

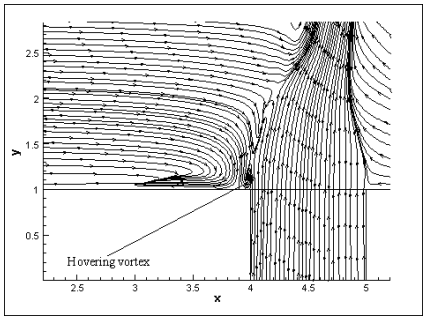


FIG 5: Streamline patterns on the vertical plane (x, y, z=3D). Close view near the jet leading edge.

## 4.2 Inclined jet in cross-flow

The influence of the streamline injection angle variations on the flow structures of JICF was assessed and again the study focuses on the flow structures and vortex dynamics.

Figures 6a, 6b and 6c present the iso-surfaces of spanwise vorticity ($\omega_z$) for 90°, 60° and 30° injection angles. Red or blue color corresponds to the positive or negative values of $\omega_z$ , respectively. It is obvious that the CRVP is present in all cases of injection angle with the shear layer (Kelvin-Helmholtz) vortices emerge at the upstream side of the initial portion of the jets. However, for 30° injection angle, as the jet is much closer to the wall the evidence Kelvin-Helmholtz rollers is less clear. At larger injection angle, the jet penetration is found to be higher and the jet spreading area is wider, as expected. The streamlines in Fig. 7 indicate that for 90° injection the blocking effect of the jet on the cross-flow is much important and the approaching cross-flow is deflected laterally to a much greater degree by the 90° jet compared to the inclined jets. This large lateral deflection has led to highest entrainment process of the cross-flow in the near wake region (at the leading edge of the jet hole). In agreement with these observations, velocity vector plot in Fig. 8 shows that the secondary flow characterizing the cross-flow entrainment in the wake region is significantly increased with the increasing of jet injection angle. This phenomenon of entrainment is of a particular importance in many engineering and industrial applications. In the film cooling of turbine blades the entrained hot cross-flow in the near wake region produces a strong local heating of blade surfaces and reduces the cooling efficiency.

It is also observed that at 30° injection angle, a pair of normal-wall vortices is formed upstream the jet hole (Fig. 7c). The possible reason for this is that since the jet and cross-flow fluids are traveling nearly parallel to each other as the jet is penetrating into the cross-flow and the velocity difference between the two parallel streams has led to the recirculation zone upstream the jet orifice.

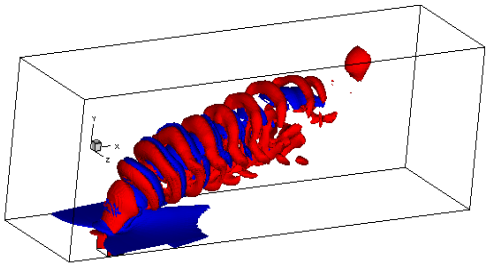

(a)

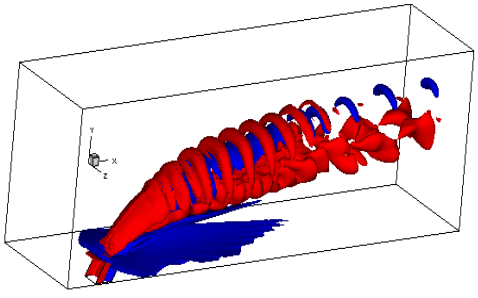

(b)

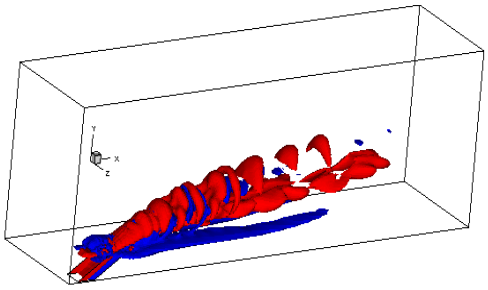

(c)

FIG 6: Simulated iso-surfaces of the spanwise vorticity ($\omega_z=0.5\ u^2/D^2$, red positive and blue negative): (a) 90° normal jet, (b) 60° inclined jet, (c) 30° inclined jet. Red or blue color corresponds to the positive or negative values of $\omega_z$, respectively.

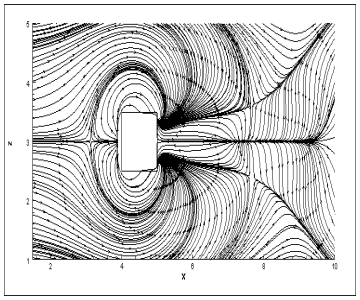

(a)

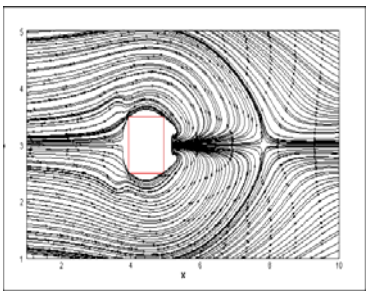

(b)

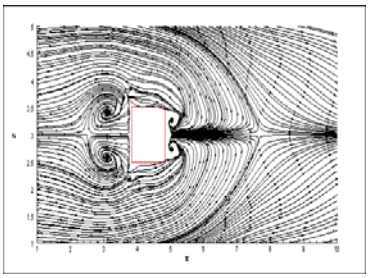

(c)

FIG 7: Streamline pattern on a horizontal plane (x, y=1.2D, z). (a), (b), (c) as defined in Fig.6.

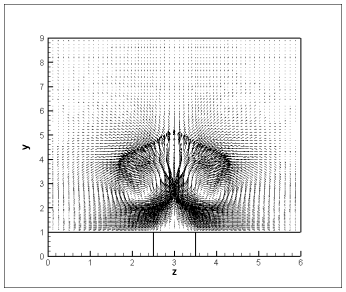

(a)

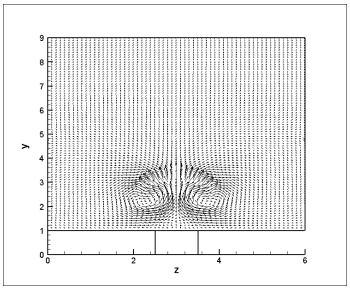

(b)

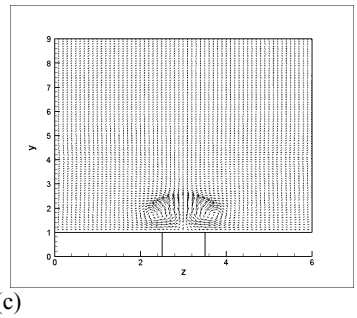

(c)

FIG 8: Vector plots at a streamwise location of x=6.5D, illustrating the CRVP shapes and the cross-flow entrainment in the wake region. (a), (b), (c) as defined in Fig.6.

The vorticity contours of $\omega_z$ are shown at location y = 1.2D from the wall (Figs. 9a-9c). Compared with the perpendicular injection case at the same blowing ratio, the starting position of the CRVP is shifted downstream and its strength is reduced at both 60° and 30° injections. For 30° injection, since the jet is much closer to the wall, the interaction between the jet and the boundary layer is more complex in the wake region. The evidence of wake vortices is not as clear in the instantaneous plots in Fig. 9c.

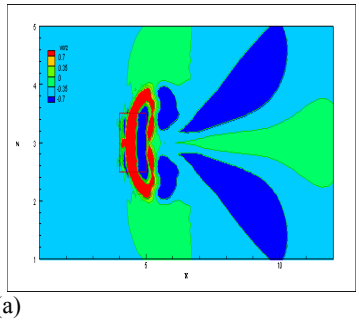

(a)

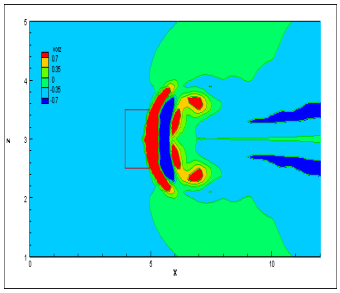

(b)

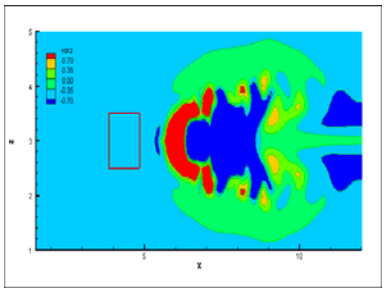

(c)

FIG 9: Simulated $\omega_z$ contours at (x, y=1.2D and z) plane. (a), (b), (c) as defined in Fig.6.

## CONCLUSIONS

The effect of the jet streamwise inclination angle on dynamical evolution of vertical structures in JICF has been studied by direct numerical simulation. The simulation reveals the vortical flow development around square jets issuing vertically into a cross-flow at the injection angles of 90°, 60° and 30°.

For normally injected jet case, the resulting vortex structures were in good agreement with both experiments and other numerical simulations in the literature. The computations successfully reproduced the important vortex patterns presented in such a flow, including the counter-rotating vortex pair, horseshoe vortex and shear layer vortex.

The jet inclination angle variations largely affect the evolution of different vortical structures and the interactions among them. Indeed, the simulation results show that the jet penetration, spreading angle and jet cross-flow mixing depend strongly on the jet inclination angle. The highest jet penetration and spreading is observed for the normal jet injection. The streamwise inclination weakens significantly the cross-flow entrainment into the near wake region and the first appearance of the CRVP is shifted downstream of the jet hole. These observations and information are of great practical relevance notably for cooling system of turbine blades designer.

## Acknowledgements

The support of the UK Engineering and Physical Science Research Council through the research grant (EP/C014979/01) is gratefully acknowledged.

*References:*

[1] Margason, R.J., Fifty year of jet in cross flow research, AGARD-CP-534, 1993, pp. 1-41.

[2] Fric, T.F. and Roshko, A.**,** Vortical structure in the wakeof a transverse jet, *J. Fluid Mech*., **279:1-47,** 1994, .

[3] Smith, S.H., Lozano, A., Mungal, M.G. and Hanson, R.K., Scalar mixing in the subsonic jet in cross-flow. AGARD-CP-534, 1993, pp. 6.1-6.13.

[4] Smith, S.H. and Mungal, M.G., Mixing structure and scaling of the jet in crossflow, *J. Fluid Mech,* **357:83-122,** 1998.

[5] Lozano, A., Smith, S.H., Mungal, M.G., Hanson, R.K., Concentration measurements in a transverse jet by planar laser-induced fluorescence of acetone, *AIAA J.*, **32:218-221**, 1994.

[6] Eiff, O.S., Kawall, J.G., Keffer, J.F, Lock-in of vortices in the wake of an elevated round turbulent jet in a crossflow. *Exps*. *Fluids,* **19:** 203-213, 1995.

[7] Lee, S.W., Lee, J.S., Ro, S.T., Experimental study on the flow characteristics of streamwise inclined jets in crossflow, *ASME J. Turbomach*., **116:** 97–105, 1994.

[8] Yuen, C.H.N. and Martinez-Botas, R.F. Film cooling characteristics of a single round hole at various streamwise angles in a crossflow: 1. effectiveness. *Int J. of Heat and MassTtransfer,* **46:** 221–235**,** 2003.

[9] Yao, Y., Lawal, A.A., Sandham, N.D., Wolton, I., Ashworth, M., Emerson, D., Massively parallel simulation of shock/boundary-layer interactions, in Proc. of Applied CFD, Beijing, China, 2000, pp. 728-735.

[10] Sandham, N.D., Li, Q., Yee, H.C., Entropy splitting for high-order numerical simulation of compressible turbulence, *J. of Comp. Phys*, **178:307-322,** 2002.

[11] Lim, T.T., New, T.H. and Luo, S.C., On the Development of Large-scale Structures of a Jet Normal to a Cross Flow. *Physics of Fluids*, **13:** 770-775, 2001.

[12] Sau, A., Sheu, T.W., Hwang, R and Yang, W.C., Three-dimensional simulation of square jets in cross-flow, *Physical Review E*, **69(6),** 2004, Art. No.066302.

[13] Kelso, R.M., Lim, T.T. and Perry, A.E., An experimental study of round jets in cross-flow. *J. Fluid Mech*., **306: 111-144**, 1996.